

PACS numbers: 42.62.Cf; 73.20.Mf; 42.65.Re
DOI: 10.1070/QE2014v044n04ABEH015376

Specific features of formation of self-induced gratings on metal foils during scanning by a tightly focused femtosecond laser beam

A.V. Dostovalov, V.P. Korolkov, S.K. Golubtsov, V.I. Kondrat'ev

Abstract. **Formation of self-induced gratings on a metal surface scanned by a focused femtosecond laser beam has been investigated. It is experimentally shown that application of femtosecond IR radiation allows one to form more ordered self-induced gratings as compared with the gratings formed by visible light. The dependence of the tilt of grating lines with respect to the beam polarisation direction on the distance between tracks and the beam motion direction in adjacent tracks is analysed. Formation of two-dimensional periodic gratings during double laser beam passage along the same trajectory but with a small difference in the beam polarisation directions has been found for the first time.**

Keywords: *femtosecond laser nanostructuring, self-induced periodic nanostructures, two-dimensional self-induced gratings.*

1. Introduction

Femtosecond laser microprocessing has become one of the most intensively developing laser technologies in the last years [1]. Surface laser ablation is widely used to form micrographs [2] and three-dimensional surfaces with minimally possible mechanical and thermal strains in the regions subjected to processing [3]. A detailed analysis of the surfaces of different materials processed by femtosecond laser radiation revealed formation of self-induced periodic nanostructures with a period smaller than the laser wavelength [4, 5]. Under these conditions, the laser beam diameter can be as large as 1 mm. It was shown that the direction of grating lines is determined by the beam polarisation direction [6, 7].

The effect of self-induced surface nanostructuring can be explained by the interference between the incident electromagnetic wave and the surface plasmons excited by this wave [8, 9]. The quantitative properties of femtosecond laser nanostructuring have been poorly investigated, and the results obtained call for further refinement. Nevertheless, even now the nanostructures formed in this way are used to change the colour of metals without colouring them [10], form antireflection coatings [11], and control wettability during fabrication of microfluidic microsystems [12]. New areas of application are intensively sought for.

Our interest in the formation of self-induced gratings is stimulated by the search for a new technology of forming polymer microfluidic microsystems based on replication of metal master dies with microchannels, produced by the LIGA technology [13]. Localised coating of the microchannel surface by nanogratings can be used to change the wettability and absorption properties of certain regions and detection zones. Surface localised nanostructuring of metal master dies produced in large amounts is more efficient than individual nanostructuring of each microfluidic chip.

The investigations were performed on a laser recording system developed jointly by research teams of Novosibirsk State University and the Institute of Automation and Electrometry (Novosibirsk). This system includes a PHAROS 6W femtosecond laser (Light Conversion Ltd) (centre wavelength of the fundamental harmonic 1026 nm, pulse duration τ = 232 fs, pulse energy $E < 0.2$ mJ, and repetition rate f = 1 kHz) and a high-precision Aerotech positioner (horizontal scan range 25 × 100 mm, scan speed up to 300 mm s^{-1}, vertical scan range 6 mm). The sample scan speed V in our experiments was varied from 0.2 to 0.5 mm s^{-1}. The laser beam was focused along the normal to the surface in all experiments. A digital camera and a LED illumination system were applied to observe the recording process and perform exact positioning of the illuminated area on the sample surface. The focused beam diameter was about 4–6 μm. The samples were galvanically grown nickel foils 20–30 μm thick. The nanostructures formed on the sample surface were investigated on a Hitachi S3400N scanning electron microscope (SEM).

In our opinion, the use of a femtosecond laser beam focused into a spot less than 10 μm in size is more promising than irradiation by a wide beam through a mask for the tasks that require only local nanostructuring of metal surface. Recording by a femtosecond beam with a polarisation vector codirectional to the beam velocity vector forms a grating structure with an average period of 820 nm. This structure (Fig. 1) is much more ordered than that recorded by a wide beam (~1 mm in diameter) with a low pulse repetition rate and an energy of about 1 mJ [11]. However, gratings with a period that is almost half the femtosecond wavelength radiation are formed in the latter case.

Since the period of self-induced gratings may be important for not only optical but also microfluidic applications, we investigated recording of self-induced gratings at a wavelength of 513 nm, suggesting that the interference nature of

A.V. Dostovalov, S.K. Golubtsov Institute of Automation and Electrometry, Siberian Branch, Russian Academy of Sciences, prosp. Akad. Koptyuga 1, 630090 Novosibirsk, Russia;
e-mail: dostovalov@iae.nsk.su;
V.P. Korolkov Institute of Automation and Electrometry, Siberian Branch, Russian Academy of Sciences, prosp. Akad. Koptyuga 1, 630090 Novosibirsk, Russia; Novosibirsk National Research State University, ul. Pirogova 2, 630090 Novosibirsk, Russia;
V.I. Kondrat'ev G.I. Budker Institute of Nuclear Physics, Siberian Branch, Russian Academy of Sciences, prosp. Akad. Lavrent'eva 11, 630090 Novosibirsk, Russia

Received 27 December 2013; revision received 19 February 2014
Kvantovaya Elektronika **44** (4) 330–334 (2014)
Translated by Yu.P. Sin'kov

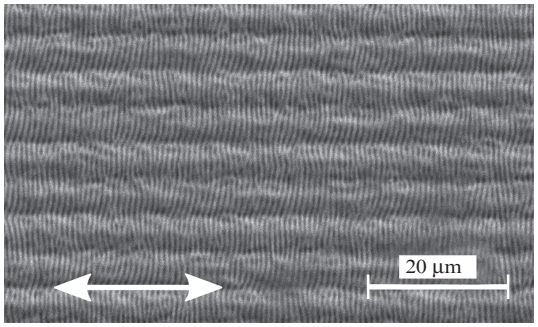

Figure 1. SEM micrograph of self-induced nanogratings recorded on the surface of a nickel foil by 1026-nm radiation with a pulse energy E = 130 nJ and scan rate V = 0.5 mm s^{-1}. The bidirectional arrow, which shows the beam polarisation direction, is located on the trajectory of laser spot centre.

this effect should lead to a proportional decrease in the period of self-induced gratings. Nickel foils moving with V = 0.2–0.5 mm s^{-1} were illuminated by a focused beam with the following parameters: τ = 270 fs, E = 130–200 nJ, f = 1 kHz, and spot diameter 6 μm. At a low pulse energy and high scan speed (12 pulses with an energy density of 0.456 J cm^{-2}), we obtained a spongy structure (Fig. 2a) with a weak periodicity in the scanning direction (along the vertical axis in Fig. 2). With an increase in the number of pulses with the same energy density (falling in an area with a size equal to the beam diameter) to 30 (V = 0.2 mm s^{-1}), pronounced linear gratings arose at the boundaries between the grooves (dark vertical areas) formed as a result of strong ablation of the surface material. The average period of nanostructures was reduced to 370 ± 20 nm, which is smaller by a factor of about 2.2 than that obtained by us in the experiments with femtosecond IR radiation having the same polarisation direction (Fig. 3a).

This pattern confirms on the whole the hypothesis explaining the formation of self-induced gratings by the interference between the light field and surface plasmons. Linear gratings are practically absent at an energy density as high as 0.71 J cm^{-2}. Thus, our experiments showed that irradiation by 1026-nm femtosecond pulses forms more uniform self-induced gratings than in the case of irradiation at the second-harmonic wavelength.

To obtain more uniform gratings, we investigated their formation at different distances between neighbouring linear tracks of the laser beam and different scan speeds. At a large distance between the tracks and a high scan speed (10 pulses, 0.54 J cm^{-2}), the self-induced grating lines were directed strictly perpendicular (Fig. 3a) to the laser beam polarisation direction (which was parallel to the scanning direction). The averaged grating period in Fig. 3a is 807 nm. With a decrease in the scan speed (25 pulses, 0.54 J cm^{-2}) (Fig. 3b), the mutual influence of tracks becomes stronger; this effect is likely of thermal origin. In the region of maximum intensity the grating is completely erased by ablation (dark bands). The lines of the gratings formed by the Gaussian beam wing during the previous passage play a role of a light-scattering (seed) structure, which stimulates the formation of surface waves with a certain phase on a wing of beam intensity distribution in the next passage. Under settled conditions, there is also a grating in the centre of the front (with respect to the motion direction) part of intensity distribution; furthermore, this grating is erased by ablation. The lines are bent or inclined as a result of these two competing processes. A similar effect of existing structures on the formation of new ones was investigated in [14], where periodic titanium oxide structures with a high degree of order (the spread of period values was ~1 nm throughout a total area of 1 mm^2) were fabricated on the surface of the titanium substrate using a positive feedback; the titanium surface between these structures remained the same. However, the formation of these structures was explained in [14] by the interference of the incident beam with the radiation scattered from the surface rather than the interaction of incident beam with excited surface plasmons.

With an increase in energy (25 pulses, 1.08 J cm^{-2}) (Fig. 3c), a deep groove is formed in the region of maximum beam intensity to isolate rather rapidly the gratings on the left and on the right from the maximum (i.e., to eliminate their mutual influence). In addition, an increase in the pulse energy rises the temperature at large distances from the impact region, thus changing the optical constants of the metal. These effects, as well as the increase in the groove wall slope, are likely to incline the grating lines. A very similar pattern, but with more ordered oblique grating lines, is observed at a pulse energy of 107 nJ (25 pulses, 0.54 J cm^{-2}) and a distance of 4 μm between tracks (Fig. 3d). When the exposure areas of neighbouring tracks are overlapped, the line direction deviates strongly from perpendicular. In addition, the rotation angle of grating lines depends on the beam scanning direction. The dark vertical areas in Figs 3c and 3d correspond to

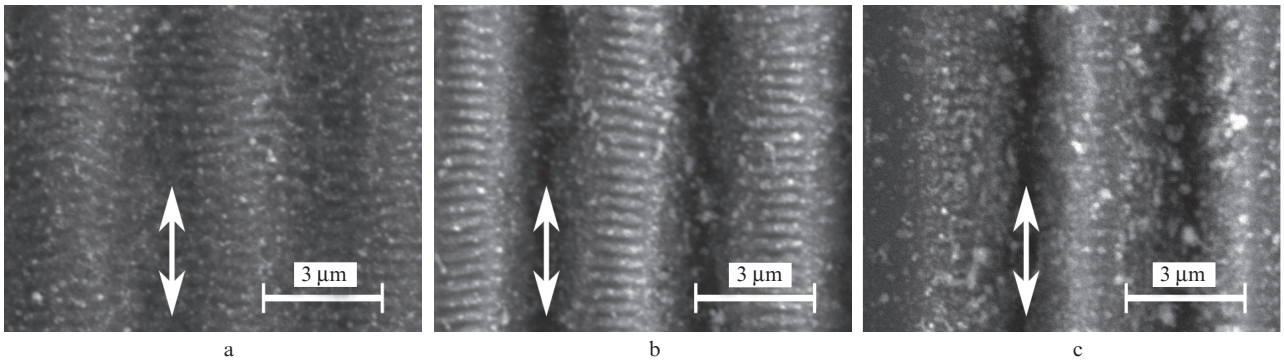

Figure 2. SEM micrographs of self-induced nanogratings recorded on the surface of a nickel foil by 513-nm radiation at different pulse energies and scan rates: (a) E = 130 nJ, V = 0.5 mm s^{-1}, (b) E = 130 nJ, V = 0.2 mm s^{-1}, and (c) E = 160 nJ, V = 0.2 mm s^{-1}. The bidirectional arrow, which shows the beam polarisation direction, is located on the trajectory of laser spot centre.

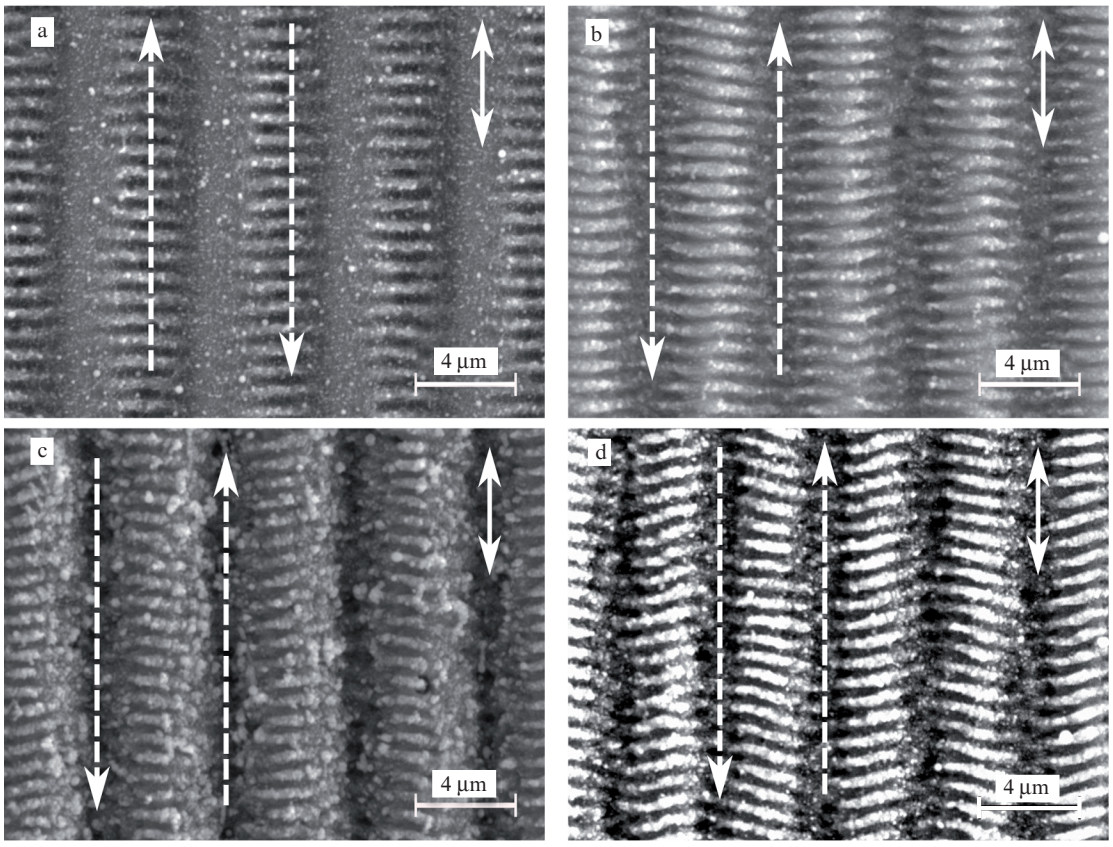

Figure 3. SEM micrographs of self-induced gratings recorded during linear scanning by a femtosecond laser beam with distances D = (a–c) 5 and (d) 4 μm between tracks, at (a) E = 107 nJ, V = 0.5 mm s^{-1}, (b) E = 107 nJ, V = 0.2 mm s^{-1}, (c) E = 215 nJ, V = 0.2 mm s^{-1}, and (d) E = 107 nJ, V = 0.2 mm s^{-1}. The bidirectional and dashed arrows show, respectively, the beam polarisation direction and the direction of beam centre motion.

the maximum of laser intensity distribution. The line rotation angle is 15°–20°. The averaged grating period in Fig. 3d along the beam motion direction is 750 nm. A similar effect of grating line rotation manifests itself in the micrographs reported in [7]. However, this effect was neither emphasised nor commented in [7], although other researchers had previously concluded that the grating lines were perpendicular to the beam polarisation direction [6]. Rotation of grooves of a self-induced grating formed on a steel surface irradiated by a picosecond laser was observed in [15]. Nanotexturing was also found to depend on the laser beam scanning direction in [15].

To study in more detail the dependence of the grating line rotation on the size of the overlap area of neighbouring tracks and the beam scanning direction, we recorded cross-shaped figures on the nickel foil surface (Fig. 4). Recording was performed during two straight-line passages of the laser beam with a small angle between the beam trajectories (14°). In Fig. 4b the beam moved in opposite directions in each successive passage (as in Figs 1–3), whereas in Fig. 4c the beam motions were codirectional. In both cases the direction of the beam polarisation vector was the same: along the first-passage direction (the y axis in Fig. 4a).

Figure 5 shows the measured dependences of the rotation angle α of self-induced-grating grooves on the distance D between tracks. The angle was measured at the midpoints of the segments between tracks with respect to the perpendicular to track 1 (the counterclockwise angle α was assumed to be positive). The change in the sign of D corresponds to the tran-

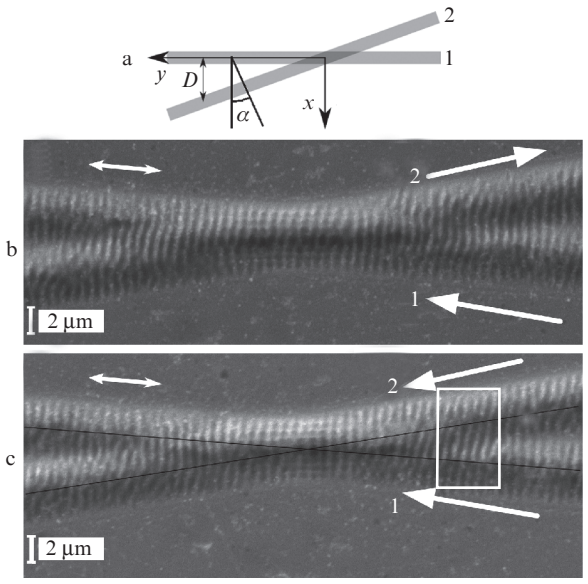

Figure 4. (a) Schematic diagram for determining the distance D between tracks and the rotation angle α of structures and (b, c) the SEM micrographs of self-induced nanogratings recorded by linear scanning of a femtosecond laser beam with different scan paths: (b) oppositely directed and (c) codirectional scans. The recording parameters are as follows: pulse energy 107 nJ, scan rate 0.2 mm s^{-1}, and wavelength 1026 nm. The arrows indicate scan directions. The bidirectional arrows show the beam polarisation directions.

sition through the track convergence point (see Fig. 4a). The measurement result was approximated by a quadratic polynomial. The maximum observed rotation angles were smaller than those in Fig. 3d. This is likely due to the deviation of the beam polarisation direction from the groove axis by 14° during the second passage. Therefore, the conditions of femtosecond irradiation are not identical in these experiments.

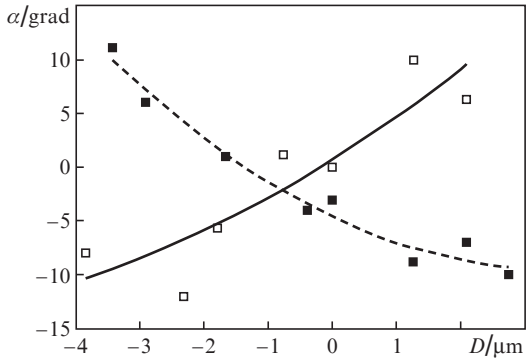

Figure 5. Dependences of the rotation angle of structures on the distance D between tracks for different scans: (□) codirectional and (■) oppositely directed.

A comparison of Figs 4b and 4c shows that the direction of scanning along neighbouring trajectories affects the character of grating line rotation. The most ordered and straight lines are formed in the case of convergence of codirectional tracks spaced by a distance $D = 2.5–3.6$ μm (the rectangle formed by white lines in Fig. 4c). In the regions where two beam tracks coincided, the main-grating lines were distinctly rotated for the opposite passage direction. Their period (800 nm) somewhat exceeds that of the gratings formed in the case of codirectional neighbouring tracks (750 nm). The subsequent divergence of the beams leads again to the formation of grating lines at a distance of 2.5–3.6 μm, which are now not straight but bent and less ordered. This can be explained by the asymmetry of distributions of the spectral or temporal characteristics of femtosecond laser beam over the cross section oriented perpendicular to the beam motion direction (an intensity distribution measurement showed its correspondence to the TEM_{00} mode).

Another possible reason is the formation (due to the ablation) of a groove with inclined walls in the first beam track. Our measurements of the relief on a white-light interferometer WLI showed that the groove depth reaches 200–300 nm. This depth corresponds to an average groove wall slope of 6°–8°. During the second passage (at some angle to the first track) the beam crosses the first groove at one side and then, after passing through the intersection point of trajectories, reaches the other groove wall. During the second passage there is a component of the polarisation vector that is perpendicular to the motion direction. At an angle of 14° between the first and second tracks, the ratio of the electric field components oriented perpendicular and parallel to the motion direction is 1:4 for the second passage. At first glance, this significant dominance of the longitudinally polarised component should completely suppress the influence of the component with transverse polarisation. However, in the portion where the tracks coincide, the presence of a weak transverse component leads to the formation of a two-dimensional grating, which can be seen in Fig. 4 (it is shown on the enlarged scale in Fig. 6). It is likely that the amplification effect is provided by the flat groove walls and grating protrusions oriented perpendicular to the walls, which were formed in the first passage. The heat sink from these protrusions is less efficient; therefore, irradiation by a large number of pulses results in a higher average temperature at their vertices, thus enhancing the interference field effect.

The formation of two-dimensional structures was revealed in [16] as a result of irradiation of a tungsten sample by two femtosecond pulses; in the interval between the pulses the sample was rotated by an angle of 90°. This effect was observed previously in [17], where irradiation of titanium through air by an immobile femtosecond beam with a wavelength of 800 nm led to the formation of two-dimensional nanogratings on the crater walls after irradiation by 10^4 pulses. The grating period depends on the beam polarisation direction: 400 nm for the nanograting with the vector $\boldsymbol{g} \perp \boldsymbol{E}$ and 1500 nm for the nanograting with $\boldsymbol{g} \parallel \boldsymbol{E}$ in the case of p-polarised radiation. In addition, formation of two-dimensional disordered structures with almost isotropic geometric characteristics was previously observed on a metal surface irradiated through a liquid layer [11]. It is of interest that the groove walls in our experiments are characterised by a small slope and that the period of nanogratings with $\boldsymbol{g} \perp \boldsymbol{E}$ (540 nm) is smaller than that of nanogratings with $\boldsymbol{g} \parallel \boldsymbol{E}$ (750 nm) by only 28%.

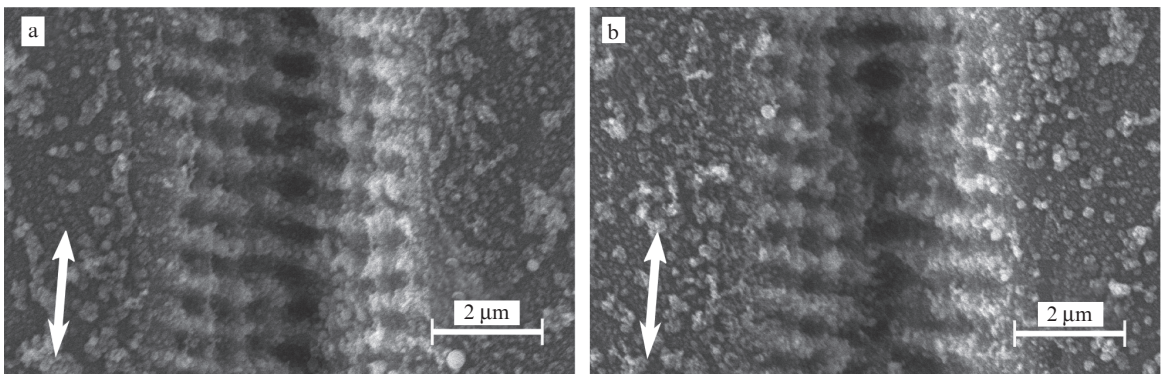

Figure 6. Enlarged SEM micrographs of self-induced nanogratings recorded during double passage of a femtosecond laser beam along the same path with different scan directions: (a) oppositely directed and (b) codirectional. The pulse energy is 107 nJ and the scan rate is 0.2 mm s^{-1}. The bidirectional arrows show the beam polarisation directions.

The profilograms (recorded on a white-light interferometer) of self-induced structures revealed a 'groove' delineating the structures formed. It was located at a rather large distance from the beam center, i.e., in the region where ablation could not occur. We concluded that this object is a swell composed of an insulator (most likely, nickel oxide) rather than a groove. The phase delay of the interferometer light beam transmitted through this swell and reflected backward leads to the same result as in the case of light reflection from a groove bottom. With allowance for the refractive index of nickel oxide (2.18), the swell height is ~20 nm. These swells are absent in the SEM photographs recorded under normal incidence of electron beam on the sample, likely because their height is smaller than that of the main relief of self-induced gratings by a factor of 10. Therefore, the difference in the electron scattering from the swell and the flat surface around it is insignificant. Apparently, nickel oxide is also formed on grating protrusions, because ablation occurs in grating grooves, as a result of which oxide is not accumulated in them. The stimulating effect of oxide layer on the formation of self-induced gratings on the titanium surface was proven in [14]. Oxidation may also be stimulating in the formation of nanogratings with $\boldsymbol{g} \perp \boldsymbol{E}$ in the presence of even a weak component of the field $\boldsymbol{E}$ oriented perpendicular to the beam scanning direction, although the oxidation activation energy for nickel greatly exceeds that for titanium.

Thus, it was experimentally shown that, with the aid of scanning by a focused femtosecond IR beam, one can form more ordered self-induced gratings than in the case of exposure to visible light. The dependence of the rotation of grating lines with respect to the beam polarisation direction on the distance between the tracks and the beam motion directions in adjacent tracks was quantitatively investigated. The formation of two-dimensional periodic gratings as a result of laser beam double passage along the same trajectory but with a small difference in the polarisation directions was revealed for the first time. Specifically, a grating was formed with a period of lines oriented along the beam motion trajectory smaller than the period of transverse lines by 28%. A possible mechanism of this effect is discussed. The use of a focused beam with a diameter of about five wavelengths allows one to obtain grooves with a large wall slope at a relatively small depth during metal ablation along the beam track. Control of the topology of self-induced gratings using different combinations of beam scanning directions along adjacent tracks, as well as the distance and angle between tracks, with a significant slope of groove walls, can be useful for local (and, possibly, anisotropic) modulation of the friction coefficient of details in micromechanical systems and for controlling microflows of liquids in microfluidic systems fabricated by replication of a locally nanostructured nickel master die with a microchannel topology.

Acknowledgements. We are grateful to S.A. Babin for the support and discussion of the results of this study.

The study was supported by the integration projects of the Siberian Branch of the Russian Academy of Sciences (Interdisciplinary Project No. 68 and Partner Project No. 92), the Russian Foundation for Basic Research (Grant No. 13-02-00805/13), and the Federal Target Programme 'Human Potential' of the Ministry of Education and Science of the Russian Federation (Agreement No. 14.132.21.1669).

References

1. Osellame R., Cerullo G., Ramponi R. *Femtosecond Laser Micromachining* (Berlin: Springer-Verlag, 2012).
2. Meunier M., Fisette B., Houle A., Kabashin A.V., Broude S.V., Miller P. *Proc. SPIE Int. Soc. Opt. Eng*., **4978**, 169 (2003).
3. Chichkov B.N., Momma C., Nolte S., Alvensleben F., Tunnermann A. *Appl. Phys. A*, **63** (2), 109 (1996).
4. Vorobyev A.Y., Makin V.S., Guo C. *J. Appl. Phys*., **101**, 034903 (2007).
5. Golosov E.V., Ionin A.A., Kolobov Yu.R., Kudryashov S.I., Ligachev A.E., Makarov S.V., Novoselov Yu.N., Seleznev L.V., Sinitsyn D.V. *Nanotechnol. Russ*., **6** (3), 237 (2011).
6. Zhao Q.Z., Malzer S., Wang L. *J. Opt. Lett*., **32** (13), 1932 (2007).
7. Dusser B., Sagan Z., Soder H., Faure N., Colombier J.P., Jourlin M., Audouard E. *Opt. Express*, **18** (3), 2913 (2010).
8. Akhmanov S.A., Emel'yanov V.I., Koroteev N.I., Seminogov V.N. *Usp. Fiz. Nauk*, **147** (4), 675 (1985).
9. Klimov V.V. *Nanoplazmonika* (Nanoplasmonics) (Moscow: Fizmatlit, 2009).
10. Vorobyev Y., Guo C. *Appl. Phys. Lett.*, **92** (4), 041914 (2008).
11. Korol'kov V.P., Ionin A.A., Kudryashov S.I., Seleznev L.V., Sinitsyn D.V., Samsonov R.V., Maslii A.I., Medvedev A.Zh., Gol'denberg B.G. *Kvantovaya Elektron*., **41** (4), 387 (2011) [*Quantum Electron*., **41** (4), 387 (2011)].
12. Wu B., Zhou B., Li J., et al. *Appl. Surf. Sci*., **256** (1), 61 (2009).
13. Dostovalov A.V., Babin S.A., Korolkov V.P., Samsonov R.V., Reznikova E.F., Goldenberg B.G. *Summaries of 15th Int. Conf. 'Laser Optics-2012'* (St.Petersburg, Russia, 2012).
14. Öktem B., Pavlov I., Ilday S., Kalaycıogly H., Rybak A., Yavas S., Erdog M., Ilday F.O. *Nat. Photonics*, **7** (11), 897 (2013).
15. Mellor L., Edwardson S.P., Perrie W., Dearden G., Watkins K. *Proc. 28th Int. Congress on Applications of Lasers and Electro-Optics (ICALEO'2009)* (Orlando, Laser Institute of America, 2009).
16. Barmina E.V., Serkov A.A., Stratakis E., Fotakis C., Stolyarov V.N., Stolyarov I.N., Shafeev G.A. *Appl. Phys. A*, **106** (1), 1 (2012).
17. Huang Y., Liu S., Li W., Liu Y., Yang W. *Opt. Express*, **17** (23), 20756 (2009).